

INVERSE PROBLEM FOR LIGHT SPREADING APPLIED TO MEDICAL TOMOGRAPHY

Project Report Version 1

Desmond Roussel Ngueguin

Under de supervision of

Emmanuel Franck, Laurent Navoret, and Vincent Vigon

CONTENT

I.	CONTEXT	3
II.	DESCRIPTION	3
1.	Objectives	3
2.	Tasks	3
3.	Resources	4
4.	Deliverables	4
III.	ROADMAP	4
1.	Mathematical basis.....	4
a.	The radiative transfer equation (RTE)	4
b.	Scheme's strengths	7
2.	Solving the model with finite volumes	7
i.	Step 1: The coupling part.....	7
ii.	Step 2: The hyperbolic part	8
3.	Analyzing the data	9
a.	Step 1: Data visualization	9
b.	Step 2: The density.....	9
c.	Step 3: The absorption and scattering opacities	9
IV.	RESULTS	10
1.	Test cases	10
i.	Case 1: transport limit	10
ii.	Case 2: diffusion limit	11
iii.	Case 3: Olson-Auer-Hall.....	12
2.	Dataframes.....	14
i.	Influence of the density	14
ii.	Influence of the absorption opacity	14

iii.	Influence of the scattering opacity	15
V.	PERFORMANCES.....	16
VI.	MILESTONES CHECK	16
VII.	PERSPECTIVES	18
VIII.	REFERENCES	18

I. CONTEXT

Inverse problems are some of the most important problems in science and mathematics because of their wide range of applications in medical imaging, computer vision, radar, etc. These are problems that, given a set of observations, tell us the parameters that cause them, parameters that we cannot directly observe. In general, numerically solving an inverse problem requires advanced optimization algorithms. However, those can be difficult to implement. That is why we are introducing an approach based on machine learning and neural networks.

The problem to solve is a medical tomography inverse problem by infrared. This project will prepare to study a neural network-based method for finding the optical properties of an organ. The project was suggested and is run by the **MOCO** ("Modélisation et Contrôle") team at IRMA ("Institut de Recherche Mathématique Avancée"). This team is made up of specialists in PDE analysis, control theory, high-performance scientific computing, and statistics (IRMA, n.d.). This specific project is under the guidance of IRMA researchers Emmanuel Franck, Laurent Navoret, and Vincent Vigon.

II. DESCRIPTION

We send an infrared light beam through an organ and we measure the signal on part of that organ. Knowing the initial conditions and the signal at all times, we can infer the influence of the organ's properties. Namely the influence of the density, the scattering opacity, and the absorption opacity. Using a P_1 model for the radiative transfer equation (1), we will implement a splitting scheme to compute the signal's value (its evolution on the boundaries of a 1-dimensional domain, and the complete signal at the end of the simulation). Then we will visually inspect the data to understand the influence of the domain's properties on the signal.

1. Objectives

Main objective:

- Find out how the optical properties of an organ affect a signal traveling through it.

Specific Objectives:

- Understand the mathematical model for radiative transfer used.
- Numerically solve the model.
- Analyze the resulting data

2. Tasks

This is a non-exhaustive list of the tasks to be completed during the project.

- Read about the mathematical model to be used (see Franck, 2012, p.169)
- Implement the splitting scheme using a finite volumes method
- Run test cases

- Analyze the data
- Write the reports
- Present the work that was done

3. Resources

The choice to use C++ to solve the P_1 model relies on it being a compiled programming language, giving us more speed, which is critically important since we will be generating thousands of lines in a dataframe to be analyzed. Python was chosen as our language for data visualization because it is simply the best at doing that. Resources used are as follows:

- [muParser](#) : a C++ library for parsing expressions into functions
- Atlas: Computing power allocated through VPN at [v100.math.unistra.fr](#)
- Google Colab: for bulk data visualization in Python

4. Deliverables

What will be delivered at the end of this project are:

- A software named **transfer** that solves the numerical model
- An analysis of meaningful trends in the data generated (notebook, pdf, ...)
- A typewritten report named **rapport_v1.pdf**
- A presentation named **presentation.pdf** (*yet to be completed*)

All these files can be found on the GitHub repository [feelpp/csmi-m1-2020-moco-inverse](#) along with instructions on how to run the software.

III. ROADMAP

1. Mathematical basis

a. The radiative transfer equation (RTE)

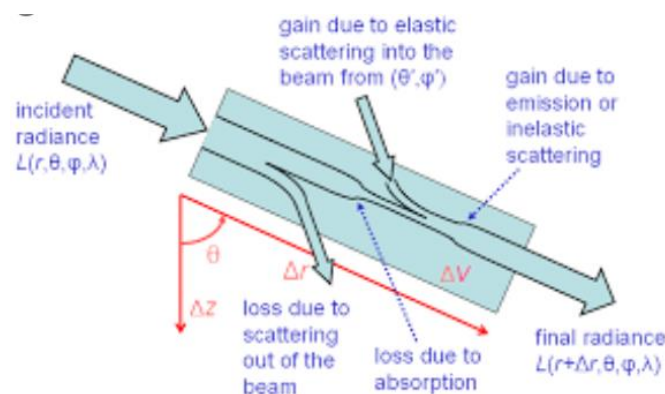


Figure 1 : Emission, absorption, and scattering phenomena in radiative transfer (Ocen Optics, n.d)

Light traveling in a straight line through a medium interacts with the matter in multiple ways (Figure 1):

- **Emission:** photons of light are emitted as a result of electrons in the matter jumping to a less excited state. This phenomenon is characterized by the emission opacity σ_e . It is the inverse of the mean length between two consecutive emissions. The matter loses energy to the light beam.
- **Absorption:** photons are absorbed by atoms and an electron (that was in an excited state) is released. This phenomenon is characterized by the absorption opacity σ_a . The matter is heated by this gain of energy.
- **Scattering:** Some photons are shifted from their direction. This phenomenon is characterized by the scattering opacity σ_c . Energy is conserved in the traveling light beam.

These opacities depend on multiple parameters among which ρ, T , and ν respectively defined as the density of the medium, the temperature, and the frequency of the photon interacted with.

We denote by $I(t, x, \Omega, \nu)$ the specific radiative intensity. As we can see, at any time t , it depends on 6 variables:

- 3 for the position x
- 2 for the direction of propagation on the photon Ω
- 1 more for the frequency of the photon ν

This quantity is directly proportionally to the number of photons found at time t in the volume dx , having a frequency in the interval of length $d\nu$, and flowing in the solid angle $d\Omega$. (Turpault, 2003).

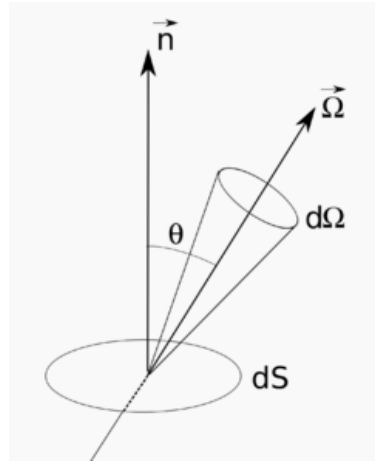


Figure 2: Solid angle used to define the specific radiative intensity

A good example of a homogeneous and isotropic intensity field is given Planck's function:

$$B(\nu, T) = \frac{2h\nu^3}{c^2} \left[e^{\frac{h\nu}{kT}} - 1 \right]^{-1}$$

Where h is Planks constant, c is the speed of light, and k is Boltzmann's constant.

A few simplifications still have to be made before we can write the radiative transfer equation (RTE). Namely that we are at the **local thermodynamic equilibrium** (LTE). That is, the local medium (at the microscopic level) is at chemical and thermal equilibrium. In this state, the opacities $\sigma_e, \sigma_a, \sigma_c$ become functions of just ρ and T .

Let's also define the **radiative equilibrium**, when the matter and the radiation are at equilibrium (namely $T_{\text{radiation}} = T_{\text{matter}}$). In this latter state, photons are distributed according to Planck's function at the medium's temperature.

The radiative transfer equation is obtained by making a summary of all the terms that affect the intensity of the light beam (absorption, emission, and scattering), at the microscopic level. We get (Franck, p.21):

$$\begin{aligned} \frac{1}{c} \frac{\partial}{\partial t} I(t, x, \Omega, \nu) + \Omega \cdot \nabla_x I(t, x, \Omega, \nu) \\ = \sigma_a(\rho, \Omega, \nu) (B(\nu, T) - I(t, x, \Omega, \nu)) \\ + \frac{1}{4\pi} \int_0^\infty \int_{S^2} \sigma_c(\rho, \Omega, \nu) p(\Omega' \rightarrow \Omega) (I(t, x, \Omega', \nu) - I(t, x, \Omega, \nu)) d\Omega' d\nu \end{aligned} \quad (\text{RTE})$$

In this equation, c is the speed of light, and p is the scattering's angular redistribution function. It is such that:

$$\oint p(\Omega' \rightarrow \Omega) d\Omega' = 1$$

It represents the probability of a photon being deviated from its original direction Ω' into our direction of focus Ω .

To obtain a kinetic P_1 model, we need to define 3 macroscopic quantities (the radiative energy, flux, and pressure) respectively as follows (Franck, p.16):

$$\begin{aligned} E(t, x) &= \int_0^\infty \frac{4\pi}{c} \int_{S^2} I(t, x, \Omega, \nu) d\Omega d\nu \\ F(t, x) &= \int_0^\infty \frac{4\pi}{c} \int_{S^2} \Omega I(t, x, \Omega, \nu) d\Omega d\nu \\ P(t, x) &= \int_0^\infty \frac{4\pi}{c} \int_{S^2} \Omega \otimes \Omega I(t, x, \Omega, \nu) d\Omega d\nu \end{aligned}$$

By computing the moment of order 1 of the RTE and taking into account that:

- The Planck function's flux is zero (since B is isotropic).
- B 's integral on all frequencies ν equals aT^4 (with $a = \frac{4\sigma}{c}$, σ being the Steffen-Boltzmann constant).

We also need to link the pressure to the energy; we then get equations (1.1) and (1.2).

Since the radiation phenomenon alone does not conserve energy, (1.1) and (1.2) need to be coupled with matter to get the conservation of energy. Luckily, we are only interested in the effects of the radiation on the matter, therefore we do not need to consider terms that are not affected by the radiation. Remembering that the probability of a photon being emitted is the same as it being absorbed (i.e. $\sigma_a = \sigma_e$ at LTE), this gives us the equation (1.3). Our P_1 model is now complete:

$$\begin{cases} \partial_t E + c \partial_x F = c \sigma_a (aT^4 - E) & (1.1) \\ \partial_t F + \frac{c}{3} \partial_x E = -c \sigma_c F & (1.2) \\ \rho C_v \partial_t T = c \sigma_a (E - aT^4) & (1.3) \end{cases} \quad (1)$$

Where:

- $a = \frac{4\sigma}{c}$ is the radiant constant

- C_v is the thermal capacity of the medium
- c is the speed of light
- $T(t, x) > 0$ is the temperature of the medium
- $E(t, x) \in \mathbb{R}$ is the energy of the photons
- $F(t, x) \in \mathbb{R}$ is the flux of the photons
- $\rho(x) > 0$ is the density of the medium
- $\sigma_a(\rho, T) > 0$ is the absorption opacity
- $\sigma_c(\rho, T) > 0$ is the scattering opacity

b. Scheme's strengths

The P_1 scheme has numerous advantages, it generalizes well under limiting conditions.

1. Transport limit

If the opacities are very weak, the photons travel through the medium without any interaction. The P_1 model keeps that property.

2. Diffusive limit

When the scattering opacity σ_c and the absorption opacity σ_a are high enough to be close to the speed of light c (which is far larger than the observed phenomenon's speed), the model in (1) is reduced to the following:

$$\partial_t(aT^4 + \rho C_v T) - \partial_x \left(\frac{c}{3\sigma_c} \partial_x aT^4 \right) = 0 \left(\frac{1}{c} \right) \quad (2)$$

This model is called the **diffusion approximation** (Franck, 2020, p.7). It matches a diffusion equation with a diffusion coefficient of $\frac{c}{3\sigma_c} \approx O(1)$.

2. Solving the model with finite volumes

Due to the hyperbolic nature of the PDE (1) and (2) in the P_1 scheme, the constraints of our domain, and the need to deal with discontinuities, the **finite volumes** method is well suited to solving it. However, the well-known Rusanov scheme is not accurate enough, especially when the opacities are very high. Therefore, we will use a finite volume scheme with a splitting strategy (Franck, 2012, p. 160).

First, we must discretize our domain to form a mesh. Let a and b be the two real numbers such that $b > a$, and $N > 0$ an integer. We split the domain $[a, b]$ into N cells of equal length to obtain a uniform mesh. At the two edges, we add two "ghost" cells. In total, we have $N + 2$ cells. Let's denote by Δx the length of the intervals (the volume of the cells). For each cell $j \in \llbracket 0, N + 1 \rrbracket$, we write x_j its center, $x_{j-\frac{1}{2}}$ its left edge, and $x_{j+\frac{1}{2}}$ its right edge.

Next, we write the splitting scheme. Two steps are required here.

i. Step 1: The coupling part

We consider the "equilibrium" part of (1). That is, the photons are not moving, and we only consider the equations that are affected by matter (i.e equations (1.1) and (1.3) where terms with temperature are involved) (Franck, 2012, p. 160). This leads to all the terms with ∂_x in (1) to be equal to 0. The equation becomes:

$$\begin{cases} \partial_t E = c\sigma_a(aT^4 - E) \\ \partial_t F = 0 \\ \rho C_v \partial_t T = c\sigma_a(E - aT^4) \end{cases} \quad (3)$$

Writing $\theta = aT^4$, we solve (3) on each independent cell. The numerical scheme is given below.

$$\begin{cases} \frac{E_j^{q+1} - E_j^n}{\Delta t} = c\sigma_a(\theta_j^{q+1} - E_j^{q+1}) \\ \frac{F_j^{q+1} - F_j^n}{\Delta t} = 0 \\ \rho_j C_v \mu_q \frac{\theta_j^{q+1} - \theta_j^n}{\Delta t} = c\sigma_a(E_j^{q+1} - \theta_j^{q+1}) \end{cases}$$

Rewritten as:

$$\begin{cases} E_j^{q+1} = \alpha E_j^n + \beta \theta_j^{q+1} \\ F_j^{q+1} = F_j^n \\ \theta_j^{q+1} = \gamma \theta_j^n + \delta E_j^{q+1} \end{cases}$$

Applying Cramer's rule, we get:

$$\begin{cases} E_j^{q+1} = \frac{\alpha E_j^n + \beta \gamma \theta_j^n}{1 - \beta \delta} \\ F_j^{q+1} = F_j^n \\ \theta_j^{q+1} = \frac{\gamma \theta_j^n + \alpha \delta E_j^n}{1 - \beta \delta} \end{cases} \quad (4)$$

Where

- E_j^n, F_j^n and θ_j^n are the value values of E_j, F_j and θ_j on the cell at the beginning of the step.
- $\alpha = \frac{1}{\Delta t} \left(\frac{1}{\Delta t} + c\sigma_a \right)^{-1}$, $\beta = c\sigma_a \left(\frac{1}{\Delta t} + c\sigma_a \right)^{-1}$, $\gamma = \frac{\rho_j C_v \mu_q}{\Delta t} \left(\frac{\rho_j C_v \mu_q}{\Delta t} + c\sigma_a \right)^{-1}$, and $\delta = c\sigma_a \left(\frac{\rho_j C_v \mu_q}{\Delta t} + c\sigma_a \right)^{-1}$
- σ_a written above is a function of ρ_j and T_j^n . Thus, it is actually $\sigma_a(\rho_j, T_j^n)$.
- μ_q is such that $\mu_q = \frac{1}{T^{3,n} + T^n T^{2,q} + T^q T^{2,n} + T^{3,q}}$

Since this step is a fixed point method, we iterate on q until we get close enough to the fixed point $(E_j^*, F_j^*, \theta_j^*)$, or more precisely (E_j^*, F_j^*, T_j^*) . We then move to the next step.

ii. Step 2: The hyperbolic part

Once the first step converges, we solve (1.2) and (1.3) as if the radiation wasn't coupled with matter. We do this with the values of E, F , and T on each cell updated from step 1. We write:

$$\begin{cases} \frac{E_j^{n+1} - E_j^*}{\Delta t} + c \frac{F_{j+\frac{1}{2}} - F_{j-\frac{1}{2}}}{\Delta t} = 0 \\ \frac{F_j^{n+1} - F_j^*}{\Delta t} + c \frac{E_{j+\frac{1}{2}} - E_{j-\frac{1}{2}}}{\Delta t} = cS_j \\ \rho_j C_v \mu_q \frac{T_j^{n+1} - T_j^*}{\Delta t} = 0 \end{cases} \quad (5)$$

With

$$\begin{aligned} F_{j+\frac{1}{2}} &= M_{j+\frac{1}{2}} \left(\frac{F_{j+1}^n + F_j^n}{2} - \frac{E_{j+1}^n - E_j^n}{2} \right), & F_{j-\frac{1}{2}} &= M_{j-\frac{1}{2}} \left(\frac{F_j^n + F_{j-1}^n}{2} - \frac{E_j^n - E_{j-1}^n}{2} \right) \\ E_{j+\frac{1}{2}} &= M_{j+\frac{1}{2}} \left(\frac{E_{j+1}^n + E_j^n}{2} - \frac{F_{j+1}^n - F_j^n}{2} \right), & E_{j-\frac{1}{2}} &= M_{j-\frac{1}{2}} \left(\frac{E_j^n + E_{j-1}^n}{2} - \frac{F_j^n - F_{j-1}^n}{2} \right) \end{aligned}$$

$$\begin{aligned}
S_j &= -\frac{1}{2} \left(M_{j+\frac{1}{2}} \sigma_{j+\frac{1}{2}} + M_{j-\frac{1}{2}} \sigma_{j-\frac{1}{2}} \right) F_j^{n+1} \\
M_{j+\frac{1}{2}} &= \frac{2}{2 + \Delta x \sigma_{j+\frac{1}{2}}}, \quad M_{j-\frac{1}{2}} = \frac{2}{2 + \Delta x \sigma_{j-\frac{1}{2}}} \\
\sigma_{j+\frac{1}{2}} &= \frac{1}{2} \left(\sigma_c(\rho_j, T_j^n) + \sigma_c(\rho_{j+1}, T_{j+1}^n) \right), \quad \sigma_{j-\frac{1}{2}} = \frac{1}{2} \left(\sigma_c(\rho_{j-1}, T_{j-1}^n) + \sigma_c(\rho_j, T_j^n) \right)
\end{aligned}$$

We must also include the CFL condition below to ensure the scheme's stability.

$$\Delta t < \frac{\Delta x}{c}$$

We can rewrite (5) as:

$$\begin{cases} E_j^{n+1} = E_j^* - A \left(F_{j+\frac{1}{2}} - F_{j-\frac{1}{2}} \right) \\ F_j^{n+1} = B F_j^* - \Gamma \left(E_{j+\frac{1}{2}} - E_{j-\frac{1}{2}} \right) \\ T_j^{n+1} = T_j^* \end{cases} \quad (6)$$

With

$$A = \frac{c \Delta t}{\Delta x}, B = \frac{1}{\Delta t} \left(\frac{1}{\Delta t} + \frac{c}{2} \left(M_{j+\frac{1}{2}} \sigma_{j+\frac{1}{2}} + M_{j-\frac{1}{2}} \sigma_{j-\frac{1}{2}} \right) \right)^{-1} \text{ and } \Gamma = \frac{c}{\Delta x} \left(\frac{1}{\Delta t} + \frac{c}{2} \left(M_{j+\frac{1}{2}} \sigma_{j+\frac{1}{2}} + M_{j-\frac{1}{2}} \sigma_{j-\frac{1}{2}} \right) \right)^{-1}$$

Once all of this is done, we move back to step 1, then back to step 2, and so on until we reach a predefined time at which we want the solution.

3. Analyzing the data

a. Step 1: Data visualization

After exporting the data from simulations in the previous step, we will need to study them using appropriate descriptive statistics tools. We will then have to find meaningful correlations between the variables. During this step, we will try to show the results that the neural network will later find by itself. The step will serve as a preparation for the AI training and predicting phase (step 2 and step 3 below), to be completed during a subsequent internship.

b. Step 2: The density

Here we will make the AI understand the trends we found in the previous step. Knowing not only the signals $E(t, x)$, $F(t, x)$, and $T(t, x)$ at all times, but also the scattering and absorption capacities ($\sigma_c(\rho, T)$ and $\sigma_a(\rho, T)$), we will rebuild the domain's density $\rho(x)$. All the inputs for the neural network will be 1D tensors (indexed either by t or by x) and the same goes for the outputs.

c. Step 3: The absorption and scattering capacities

This step is quite similar to the previous step with the only difference that we will be trying to predict $\sigma_c(\rho, T)$ and $\sigma_a(\rho, T)$ with $\rho(x)$ known. However, it requires a more complex neural network.

Just as the previous step, this part is no longer part of the project, we will cover it during the internship.

IV. RESULTS

1. Test cases

i. Case 1: transport limit

This test case corresponds to the transport limit. Except that we are interested in the signals $E + F$ and $E - F$. To perform this test, we take $\sigma_a = \sigma_c = 0$ and the initial condition for E is a gaussian distribution with its pic at the center of the domain. All the parameters for the problem are indicated in the configuration ***src/config/case_1.cfg***. Those parameters are repeated below:

```
x min 0
x max 1
N 100
c 1
a 1
c_v 1
CFL 0.99
precision 1e-4
t 0
c f 0.5
rho 1
sigma a 0
sigma c 0
E 0 exp(-(x-0.5)^2/(2*(0.05^2)))
F 0 0
T 0 1
E_l neumann
F_l neumann
T_l neumann
E_r neumann
F_r neumann
T_r neumann
E exact 0
F exact 0
T exact 0
export spatial data/df spatial.csv
export temporal data/df temporal.csv
```

Figure 3: Configurations for the transport test case. The “neumann” term indicates the natural flow condition on the boundaries.

Detailed instructions on writing a configuration file are given in the ***README.md*** file at the root of the github repo associated with this project. Now, the next step is to run the program using the command ***build/transfer src/config/case_1.cfg*** and visualize the results in ***data/case_1_spatial.csv***.

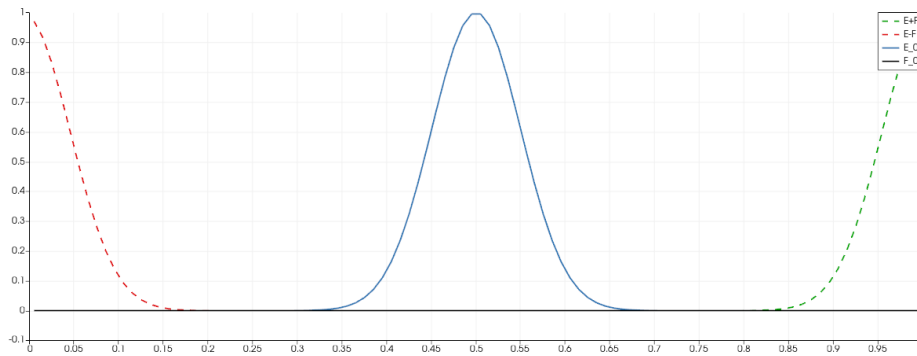


Figure 4: Transport test case. $E+F$ is transported at the speed $c=1$ while $E-F$ is transported at the speed $-c=-1$

ii. Case 2: diffusion limit

We will now test the diffusion limit. With the scattering opacity and the speed of light taken considerably greater than the absorption opacity ($\sigma_a = 0$ and $\sigma_c = c = 1000$), the final photon energy E should be the fundamental solution of the diffusion equation:

$$\begin{cases} \frac{\partial}{\partial t} E(t, x) - \frac{\partial^2}{\partial x^2} E(t, x) = 0, & t > 0, x \in [0, 1] \\ E_0(x) = E(0, x) = \delta_0(x) \end{cases}$$

Written as:

$$E(t, x) = \frac{1}{\sqrt{4\pi t}} e^{-\frac{x^2}{4t}}$$

There is a problem though, placing a Dirac function is difficult computer-wise (since it equals $+\infty$ on its domain). To solve this, we modify that initial conditions by shifting the time axis by $t_0 = 0.002$. The initial condition becomes:

$$E_0(x) = E(t_0, x) = \frac{1}{\sqrt{4\pi t_0}} e^{-\frac{x^2}{4t_0}}$$

Configurations for this test case are given below:

```
c 1000
sigma c 1000

x_min 0
x_max 1
N 100

a 1
C_v 1
CFL 0.99
precision 1e-6
t_0 0.002
t_f 0.02

rho 1
sigma_a 0

E_0 exp(-(x-0.5)^2/(4*1*(t_0)))/(2*sqrt(_pi*1*(t_0)))
F_0 0
T_0 0

E_exact exp(-(x-0.5)^2/(4*1*(t+t_0)))/(2*sqrt(_pi*1*(t+t_0)))
F_exact 0
T_exact 1

E_l neumann
F_l neumann
T_l neumann

E_r neumann
F_r neumann
T_r neumann

export_spatial data/df_spatial.csv
export_temporal data/df_temporal.csv
```

Figure 5: Configurations for the diffusion limit test case

After running the command **build/transfer src/config/case_1.cfg**, the results will be exported into **data/case_2_spatial.csv** and **data/case_2_temporal.csv**.

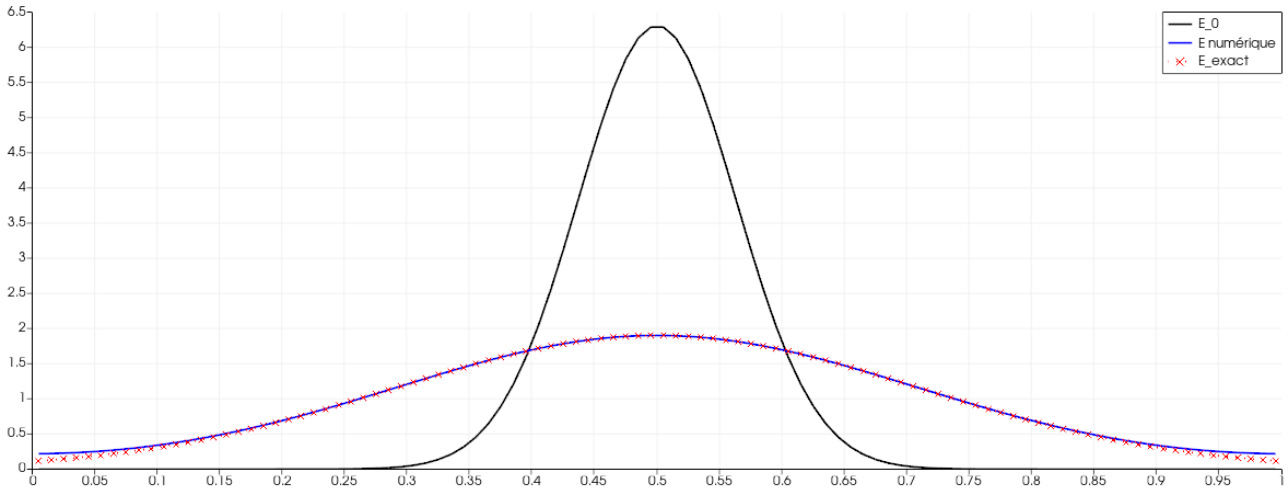


Figure 6: Spatial visualisation of the numerical and the exact solution for the diffusion limit

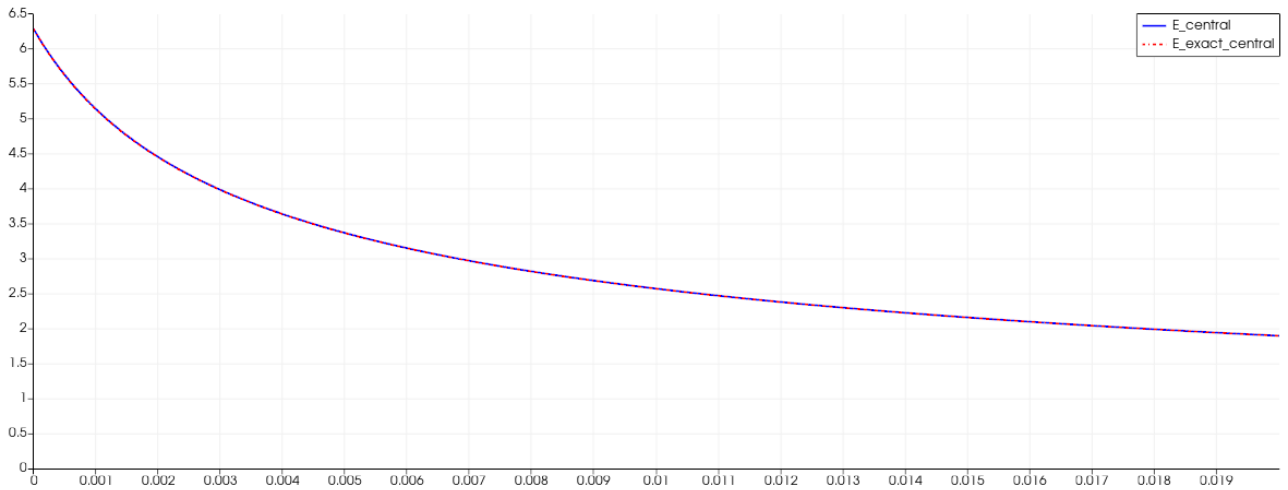


Figure 7: Temporal decrease in energy at the center of the domain for the diffusion limit

As we can see and hoped, our computed solution (in solid line) perfectly matches the expected solution (in dashed line).

iii. Case 3: Olson-Auer-Hall

Contrary to the previous test cases, this one focuses on temperature. It tells the evolution of the radiation and the medium's temperature. The domain $[0,3]$ is heated by a blackbody to the left (with $T_r = 0.056234 \text{ keV}$). As the body gets hotter, its absorption opacity increases, causing thermal equilibrium between the radiation and the mater (Franck, 2012, p.171).

```

rho 0.056234
sigma_a 0.01003/(T^3)
sigma_c 0

x_min 0
x_max 3
N 100

c 299
a 0.01372
C_v 0.14361
CFL 0.25
precision 1e-6
t_0 0
t_f 0.00334448

E_0 0.056234^4
F_0 0
T_0 0.056234

E_1 0.01372*1^4
F_1 0
T_1 1

E_r neumann
F_r neumann
T_r neumann

E_exact 0
F_exact 0
T_exact 0

export_temporal data/df_temporal_olson.csv
export_spatial data/df_spatial_olson.csv

```

Figure 8: Configuration for the Olson-Auer-Hall test case

The results below are plotted in log scale for the abscissa x .

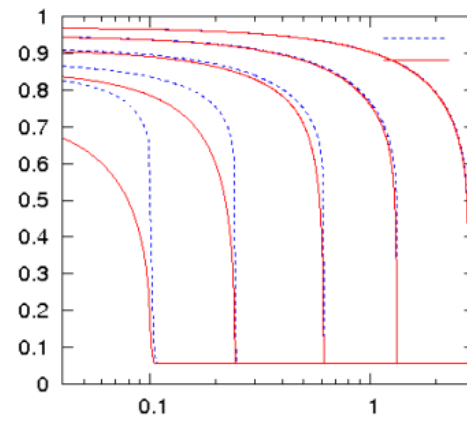


Figure 9: Expected results for $t=1/c$, $3/c$, $10/c$, $30/c$, and $100/c$ (Franck, 2012, p.171)

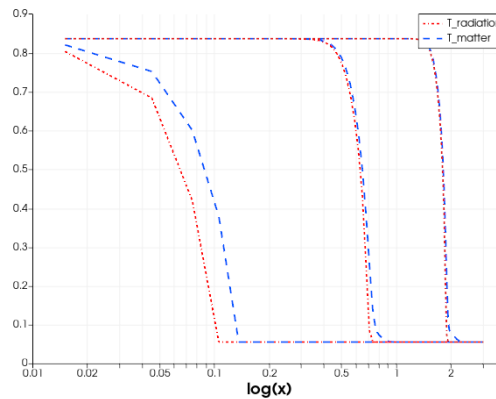


Figure 10: Obtained results for $t=0.1/c$, $1/c$, and $3/c$

As we can see, the result doesn't match the reference. This problem is yet to be corrected.

2. Dataframes

The notebook [src/notebook/analyse_des_donnees.ipnb](#) analyses data (in the form of dataframes) created from the program, and explains some trends (the [Colab version](#) is recommended as the Jupyter version indicated above is stored locally in the repository and will easily run into errors). We repeat some of the results below. The data has been created with the bash script [src/simu/gauss_dump.sh](#). Apart from ρ , σ_a and σ_c that change, the remaining parameters are constants. Particularly, the initial value of the signal E is the same gaussian function we used in the test case 1. Initial values for F and T are respectively 0 and 1.

i. Influence of the density

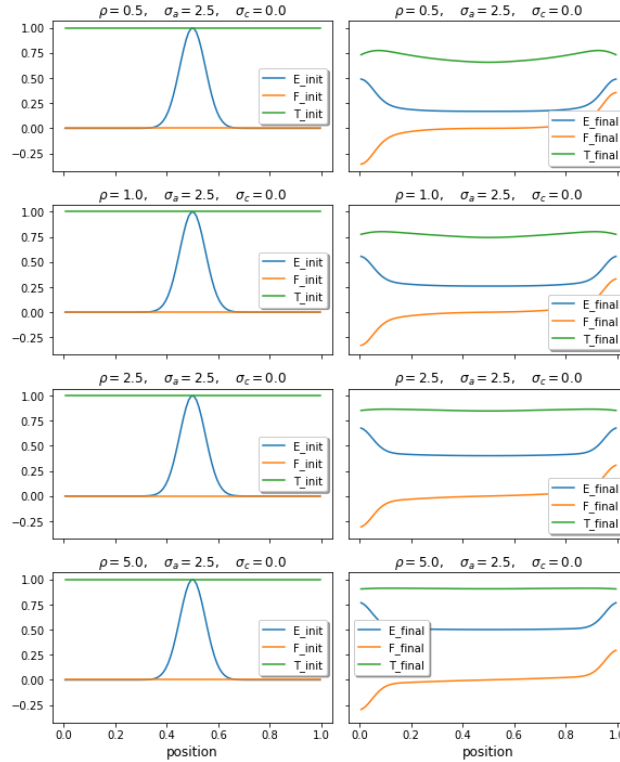


Figure 11: Influence of the density on E , F , and T for $\sigma_a = 2.5$ and $\sigma_c = 0$

It seems that as the density increases (Figure 12):

- The radiative energy E increases
- It doesn't change the flux F
- The temperature varies less. The equilibrium temperature seems to be higher.

ii. Influence of the absorption opacity

It might be that as the opacity σ_a increases (Figure 11):

- The diffusion phenomenon is faster, but the energy E keeps the same pic value
- The flux F is attenuated during transport
- The temperature change is more important, and the thermal equilibrium is faster

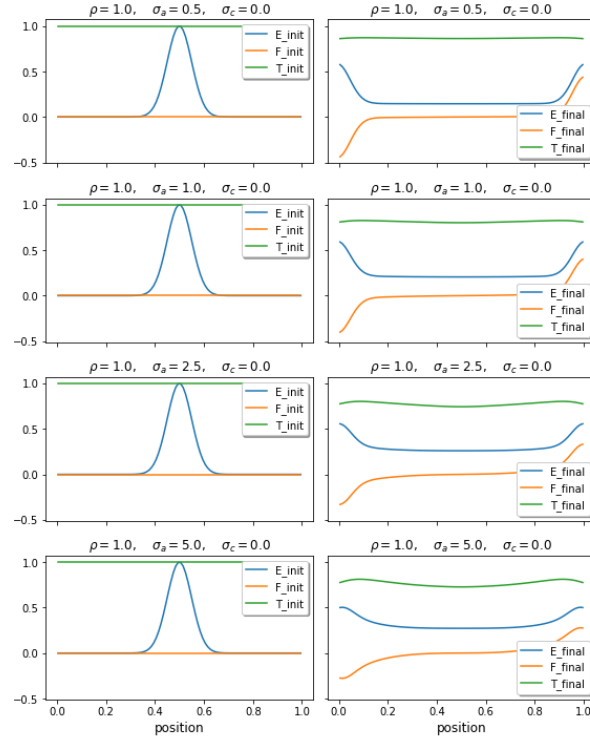


Figure 12: Influence of σ_a for $\rho = 1$ and $\sigma_c = 0$

iii. Influence of the scattering opacity

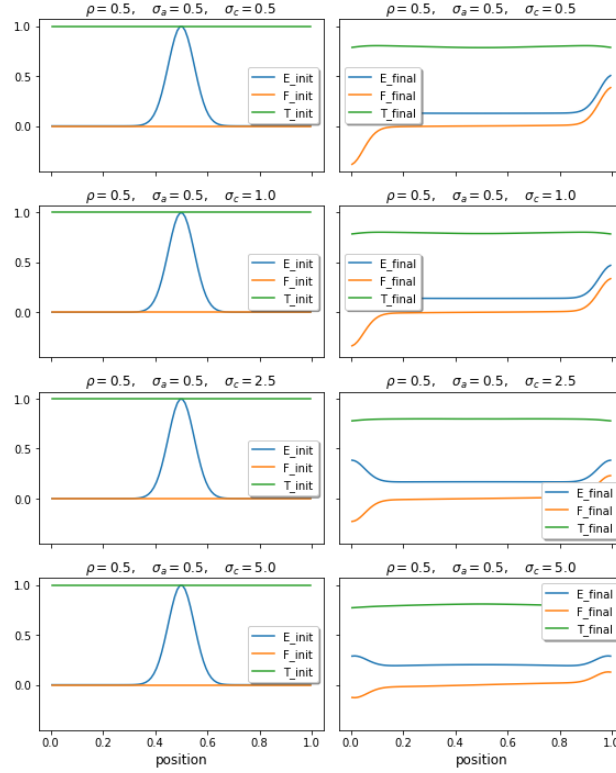


Figure 13: Influence of σ_c for $\rho = 0.5$ and $\sigma_a = 0.5$

From figure 13, it seems obvious that an increase in σ_c decreases the values of both the energy and the flux. However, to the naked eye, it's less obvious to notice any change in temperature.

Of course, these are but conjecture. Plus, the opacities usually change with the density and temperature of the medium (see test case 3). This means that their form is not as simple as constants as we assumed. However, this simple analysis shows potential trends that might be confirmed or invalidated by a convoluted neural network.

V. PERFORMANCES

Speed is very important in this problem. Especially since we plan on generating a huge amount of data to be analyzed (potentially millions of lines of signals). Earlier versions of the program *transfer* lacked the speed necessary to do so. The program was bloated by external libraries, especially the ones for parsing string expressions into functions. The problem has since been solved by changing from *exprtk* to *muParser*. Moreover, other optimization steps that can be viewed in the code for the *Solver* class have proven efficient.

VI. MILESTONES CHECK

This section gives a summary of the roadmap, the tasks, the goals, and the deadlines for the project. Original estimates were written in black, and new estimates are marked in red.

Milestone		Details	Tools needed	Deadline	Estimated number of hours	Effective number of hours
Understanding the model		We will seek to understand the PDE (1) and its numerical model on a slightly theoretical basis. This has already been done, but new information keeps coming every day.		April 2, 2020	8 hours	20 hours
Report version 0		A report indicating the context and the roadmap for the project. This milestone is currently under completion.	MS Word	April 15, 2020	16 hours	32 hours
<u>Solving the splitting scheme</u>	Solving the scheme	Using the finite volumes method in 1D, we need to solve the PDE (1). This has milestone has already been completed.	VS Code, GitHub, Eigen , Csparse <i>muParser</i>	April 15, 2020	40 hours	60 hours
	Verification	Verify that the finite volume method is correctly implemented and solves a direct problem on a given domain. A good way to verify our splitting scheme is to test it on the diffusion approximation in (2). Tests will be put in place for continuous integration. We will	VS Code <i>Paraview</i>	April 29, 2020	16 hours	60 hours

		need to find and correct all the bugs that appear in the code.				
	Benchmarking	Compare our algorithm to known solutions to optimize our code for speed. This step might be done multiple times depending on the changes we make to the algorithm during verification.	VS Code	April 29, 2020	4 hours	4 hours
	Validation	Making sure the problem solves the correct direct problems linked to medical tomography.	VS Code Paraview	April 29, May 22, 2020	4 hours	16 hours
	Data export	Writing and running a script that exports thousands of instances of a correctly solved direct problem. We will make sure to export the data <u>one state of the model at a time</u> . This requires us to run the above-optimized program a great number of times, which is the reason we need to get it right on the first try.	Altas	May 5, 2020	8 hours	16 hours
Analyzing the data	Studying the data	Using the exported data, we will seek to learn new information, finding interesting correlations, creating new variables, deleting outliers, cleaning out the data, and so on. During the internship, our goal will be to make the AI understand these correlations.	Google Colab Jupyter	May 19, 2020	24 hours	8 hours
	Verification	Verify that the model is properly studied. A positive indicator might be that when generating new instances of the data, we continue seeing the same trends.	Google Colab Jupyter	May 19, 2020	16 hours	4 hours
	Validation	Check that the trends we find are effectively the trends from light spreading in medical tomography. We will compare our data trends to known databases in the same area of study.	Google Colab Jupyter	May 19, 2020	4 hours	--
	Benchmarking	Check that our algorithms for analysis are fast enough to be easily repeatable on other systems.	Google Colab	May 19, 2020	4 hours	--
Report version 1		The task is to write a more complete version of the report.	MS Word	May 19 22, 2020	8 hours	16 hours
Report version 2		The final version of the report, incorporating corrections indicated by the supervisors.	MS Word	May 19 27, 2020	4 hours	--
Presentation		A slideshow to be written in PowerPoint.	MS PowerPoint	May 19 28, 2020	8 hours	--

The initial estimates to be spent on the projet was **164 hours** (approximately 7 full days. However, the effective time spent on the project (which is yet to be completed) is closer to **232 hours** (or 10 full days).

VII. PERSPECTIVES

The project has led us to see how their energy is affected when photons travel through a medium (test cases 1 and 2). We have also been able to observe how the radiative temperature evolves as it travels through a medium at radiative equilibrium (test case 3). The satisfying results encourage us to generate more data. In a follow up to this project, we could train a neural network that will then predict the optical properties of the medium.

That said, it is important to note that our numerical scheme heavily depends on the P_1 model for the radiative transfer equation. While not costly and relatively easy to solve, the P_1 model has a major disadvantage: it only gives predictions when the anisotropy factor (normally $f \leq 1$) is reduced, i.e:

$$f = \frac{\|F\|}{cE} \leq 0.57 \quad (\text{Turpault, 2003, p.22})$$

Hence the lamination of the flux, one of the radiative transfer's most fundamental properties might not be satisfied. This shortcoming will be addressed during an internship and other methods like the P_n , or M_1 model will be tested.

VIII. REFERENCES

- Franck, E. April 1, 2020. "*Projets de M1*". Personal notes from Emmanuel Franck summarizing the guidelines for the project.
- Franck, E. October 23, 2012. "*Construction et analyse numérique de schéma asymptotic preserving sur maillages non structurés. Application au transport linéaire et aux systèmes de Friedrichs*". Retrieved from <https://tel.archives-ouvertes.fr/file/index/docid/744371/filename/theseFranckv3.pdf>
- IRMA. (n.d.). "*Institut de Recherche Mathématique Avancée, UMR 7501*". Retrieved from <http://irma.math.unistra.fr/rubrique162.html>
- Turpault, R. 2003. "*Modelisation, approximation numerique et applications du transfert radiatif en desequilibre spectral couple avec l'hydrodynamique*". Mathématiques [math]. Université Sciences et Technologies - Bordeaux I, 2003. Français. tel-00004620